

Supplementary Tables and Figures to

Hexosylceramides are elevated in human, mouse and cellular Parkinson's disease and cause gene upregulations in neurons mimicking responses to pathogens

Luisa Franck¹, Lisa Hahnefeld^{1,2}, Lucie Valek¹, Katharina Klatt-Schreiner¹, Annett Wilken-Schmitz¹, Mohamad Wessam Alnouri³, Sandra Trautmann^{1,2}, Marc-Philipp Weyer¹, Dominique Thomas^{1,2}, Robert Gurke^{1,2}, Stefan Offermanns³, Gerd Geisslinger^{1,2}, Irmgard Tegeder¹

¹Goethe University Frankfurt, Faculty of Medicine, Institute of Clinical Pharmacology, Theodor-Stern-Kai 7, 60590 Frankfurt am Main, Germany.

²Fraunhofer Institute for Translational Medicine and Pharmacology ITMP and Fraunhofer Cluster of Excellence for Immune Mediated Diseases CIMD, Theodor-Stern-Kai 7, 60596 Frankfurt am Main, Germany

³Max Planck Institute for Heart and Lung Research, Department of Pharmacology, Bad Nauheim, Germany

Supplementary Tables

Suppl. Table 1: Demographic data for plasma lipidomic analyses

Demographic data - Samples for plasma lipidomic analyses. Modified from Mov Disord. 2020 Oct;35(10):1822-1833. doi: 10.1002/mds.28186.

Demographic data

	Healthy controls (HC)				Parkinson's Disease (PD)			
	female (n = 25)		male (n = 25)		female (n = 16)		male (n = 34)	
	Mean	SD	Mean	SD	Mean	SD	Mean	SD
Age (years)	60.56	7.10	65.28	9.00	64.06	8.64	68.15	7.75
BMI	26.51	4.95	27.84	4.43	25.61	4.68	26.61	3.93
Disease Duration (years)					6.00	5.55	8.85	7.48
VAS Avg. pain	2.24	2.18	0.95	1.80	3.89	1.95	3.37	2.73

Medication		Healthy controls (HC)						Parkinson's Disease (PD)						Counts	
		female			male			female			male			Sum HC	Sum PD
		Age Class			Age Class			Age Class			Age Class				
		<= 60	61 - 70	70+	<= 60	61 - 70	70+	<= 60	61 - 70	70+	<= 60	61 - 70	70+		
Levodopa	no	13	9	3	9	7	9	2	0	1	2	1	4	50	10
Carbidopa	yes							4	5	4	6	8	13		40
DA agonists	no	13	9	3	9	7	9	2	2	3	1	2	6	50	16
	yes							4	3	2	6	7	10		32
Amantadin	no	13	9	3	9	7	9	6	4	5	7	7	11	50	40
	yes							0	1	0	0	2	5		8
MAOB Inhibitors	no	13	9	3	9	7	9	1	4	2	4	5	9	50	25
	yes							5	1	3	3	4	7		23
COMT Inhibitors	no	13	9	3	9	7	9	4	4	5	5	6	10	50	34
	yes							2	1	0	2	3	6		14
Anticholinergics	no	13	9	3	9	7	9	6	5	5	7	7	16	50	46
	yes							0	0	0	0	2	0		2
HoehnYahr	0.0	13	9	3	9	7	9	0	0	0	0	1	0	50	1
	1.0							2	2	1	0	0	2		7
	2.0							3	0	1	3	2	4		13
	2.5							0	1	2	0	1	4		8
	3.0							1	2	1	4	3	4		15
	4.0							0	0	0	1	2	3		6
Pain	no	7	3	1	7	6	6	0	0	1	4	4	4	30	13
	yes	6	6	2	2	1	3	6	5	4	4	5	13	20	37
Pain medication	no	11	6	1	7	4	4	3	3	4	6	5	9	33	30
	yes	2	3	2	2	2	5	2	2	1	2	4	8	16	19

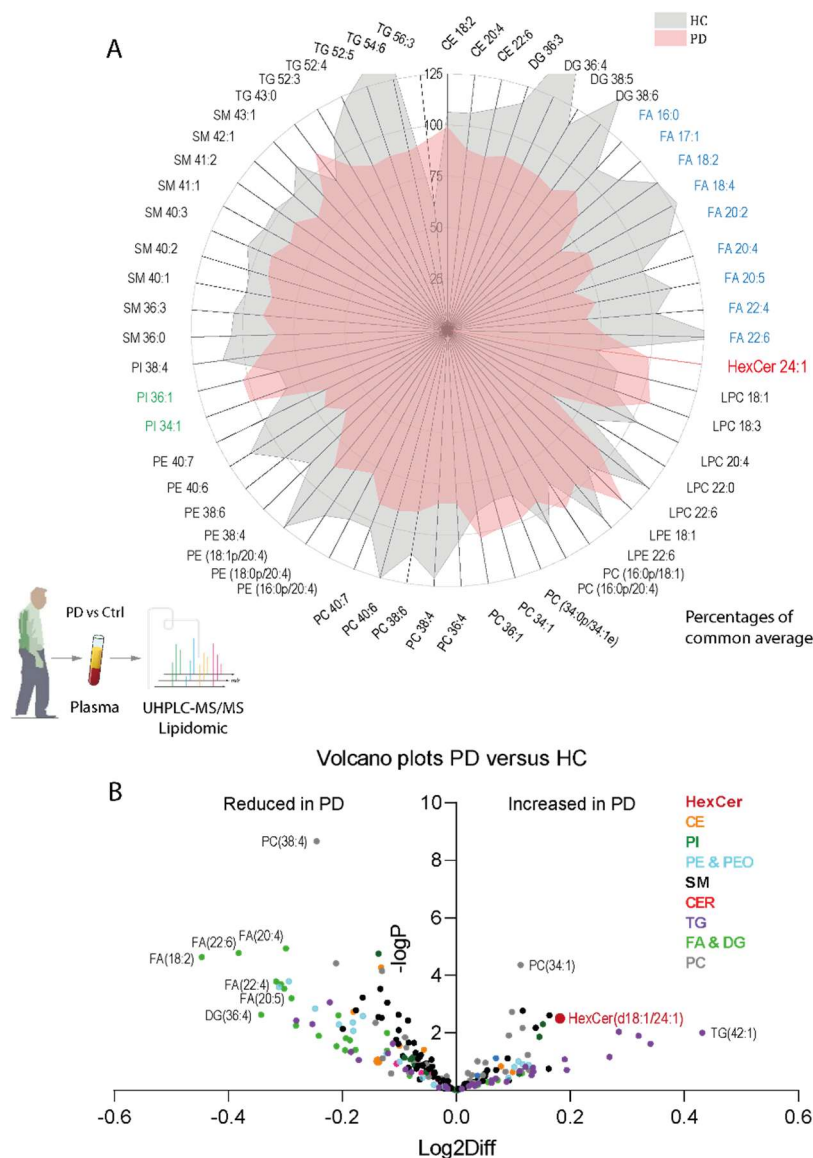
Suppl. Table 2: Demographic data of skin biopsy donor PD patients

GR	Age	sex	Sample-Veh	Sample-PIM	HoehnYahr	Disease (years)	L-DOPA	DR-agonist	MAOB-I	COMT-I	NMDA	ACH	ApoMOR	DBS
PD	61	f	PD_veh_f_JH	PD_PIM_f_JH	1.5	1	no	no	yes	no	no	no	no	no
PD	55	f	PD_veh_f_KP	PD_PIM_f_KP	1		no	yes	no	no	no	no	no	no
PD	64	m	PD_veh_m_FB	PD_PIM_m_FB	3	26	yes	yes	no	yes	yes	no	yes	no
PD	75	m	PD_veh_m_HJI	PD_PIM_m_HJI	3	7	yes	no	no	no	no	no	no	no
PD	59	f	PD_veh_f_HS	PD_PIM_f_HS	4	11	yes	no	no	yes	no	no	no	yes
PD	56	f	PD_veh_f_EM	PD_PIM_f_EM	1	3	no	yes	yes	no	no	no	no	no
PD	78	m	PD_veh_m_OH	PD_PIM_m_OH	3	21	yes	yes	no	yes	no	no	no	yes
PD	79	m	PD_veh_m_GRM	PD_PIM_m_GRM	3	16	yes	no	yes	yes	no	no	no	no
PD	72	m	PD_veh_m_GS	PD_PIM_m_GS	2	2	no	yes	no	no	no	yes	no	no
PD	84	m	PD_veh_m_MG	PD_PIM_m_MG	2	4	yes	yes	no	no	no	no	no	no
PD	58	m	PD_veh_m_TSCh	PD_PIM_m_TSCh	3	10	yes	no	no	yes	no	no	no	yes
PD	74	m	PD_veh_m_RK	PD_PIM_m_RK		3	no	yes	no	no	no	no	no	no
PD	65	m	PD_veh_m_HJB	PD_PIM_m_HJB			yes	no	no	no	no	yes	no	no

Supplementary Figures

Suppl. Fig. 1

Untargeted lipidomic screen



Supplementary Figure S1

Plasma lipidomic analyses in PD patients versus healthy controls (HC)

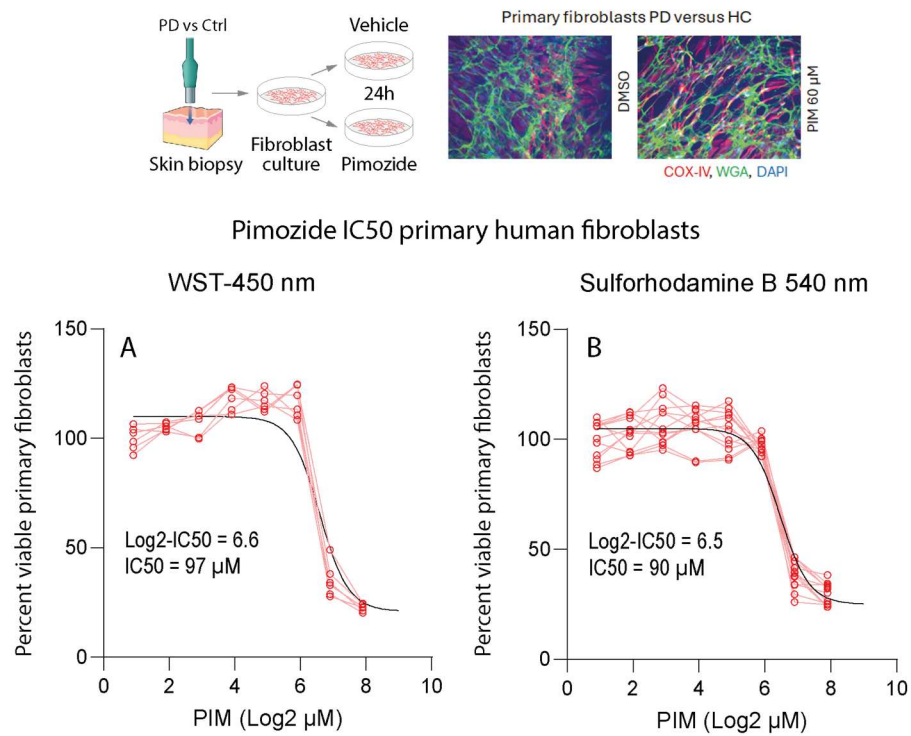
Parkinson's Disease (PD) patients (n = 16 female, 34 male) and healthy controls (HC) (n = 25 female, 25 male) were age matched 60-70+ years old at the time of blood sampling. Demographic details as in {Klatt-Schreiner, 2020 #415}.

A: The radial plots shows top down- and upregulated lipids in PD versus HC. Mass spectrometry area under the curve (AUC) were divided by the AUC of the internal standard (IS) (AUC/IS). Because lipid abundance varies over several orders of magnitude, AUC/IS values were transformed into percentages versus a common average for each lipid. The mean percentages per group are presented in the radial plot. For clarity, the plot shows no error bars.

B: Volcano plots show the Log2(fold change) on the x-axis versus the negative Log10 of the P-value of t-tests on the Y-axis. The lipid classes are colour coded.

Abbreviations: CAR, carnitines; CER, ceramides; CE, cholesterol ester; DG, diglycerides; FA, fatty acids; HexCer, hexosylceramides; LPC, lysophosphatidylcholines; LPE, lysophosphatidylethanolamines; LPG, lysophosphatidylglycerols; LPI, lysophosphatidylinositols; PC, phosphatidylcholines; PE, phosphatidylethanolamines; PD, phosphatidylglycerols; PI, phosphatidylinositols; SM, sphingomyelins; ST, sterols; TG, triglycerides; UbiQ, ubiquitin; -O ether bound.

Suppl. Fig. 2

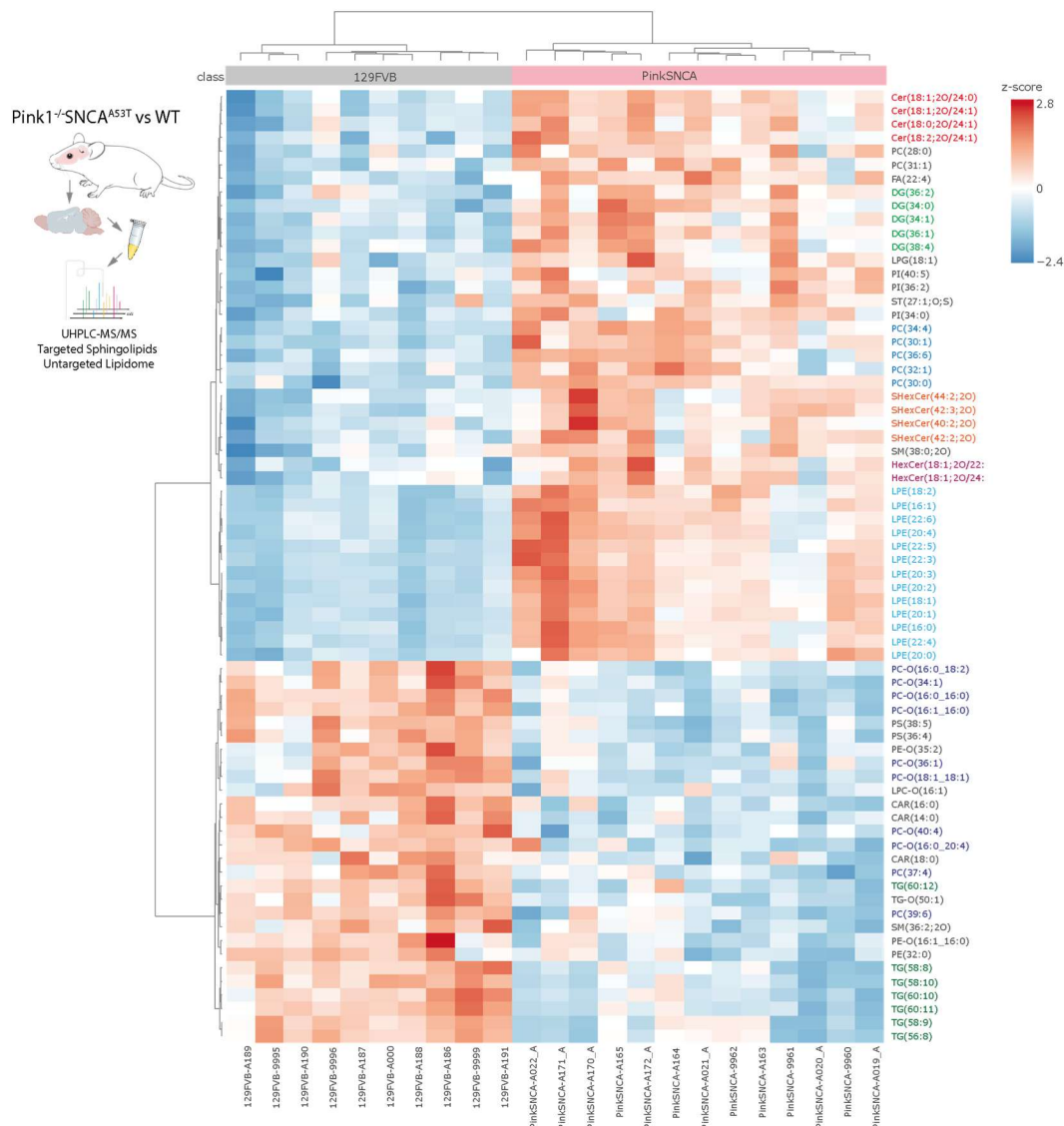


Supplementary Figure S2

Pimozide IC₅₀ in primary human fibroblasts

In a 96-well plate, PHF cultures were treated for 24h with pimozide at increasing log₂-scaled eight concentrations in rows A-H. Viability was assessed at 24h using WST reagent and sulforhodamine B (SRB) assays. WST absorbance and SRB absorbance were transformed into percentage survival as compared to the average of vehicle treated cultures and plotted on the Y-axis versus the Log₂ pimozide concentration on the X-axis. Each scatter represents one culture. The red lines connect cultures in one column of the 96-well plate. Data were analysed using as standard sigmoidal inhibitory Emax model. The fit line is shown in black. The IC₅₀ of pimozide was 90-100 μ M.

Suppl. Fig. 3 Lipidomic analysis brain tissue top 70

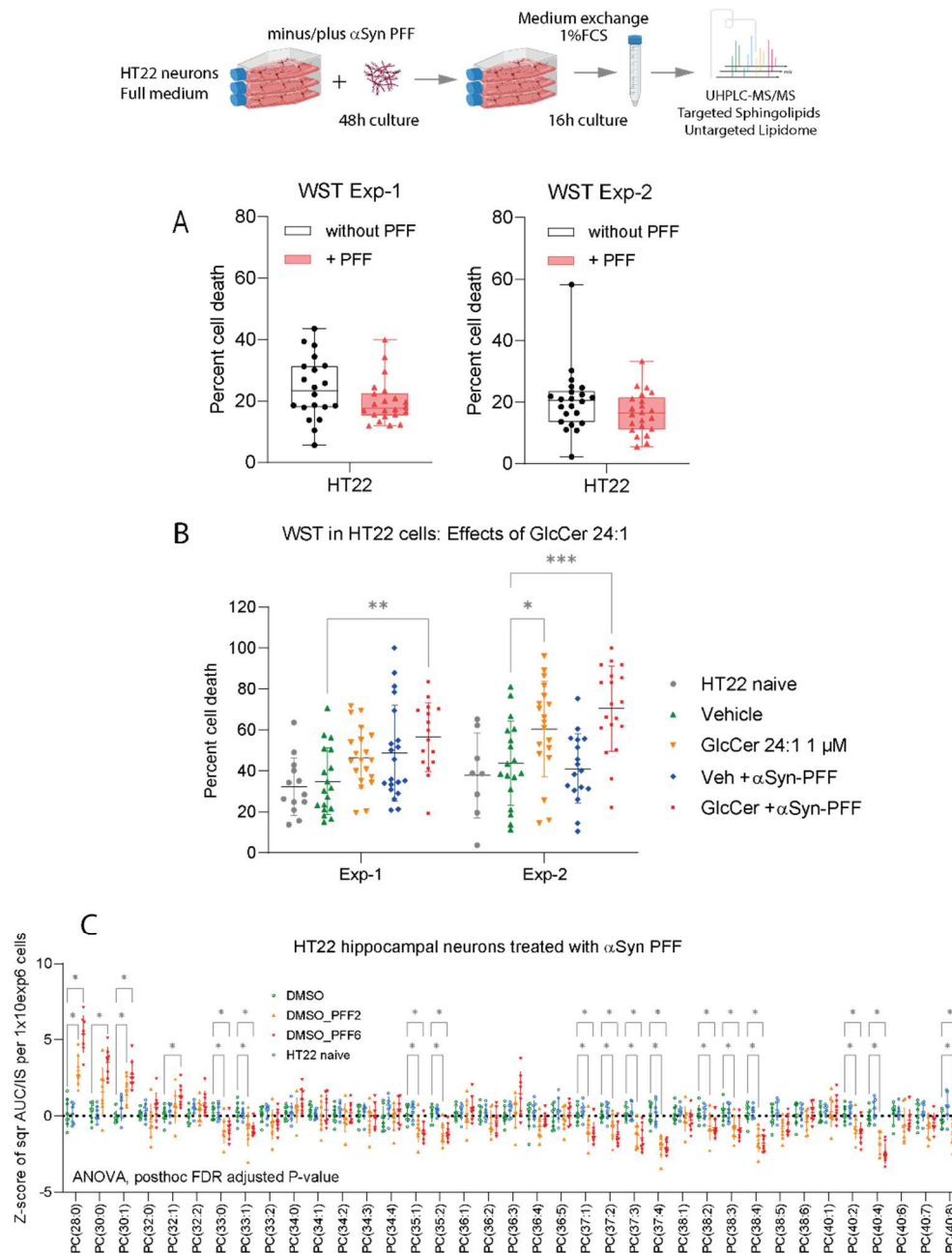


Supplementary Figure S3

Lipidomic UHPLC-MS/MS analysis of mouse brain in Pink1^{-/-}SNCA^{A53T} mice and WT controls

Heatmap of top 70 regulated lipids in Pink1^{-/-}SNCA^{A53T} mouse brain versus wildtype controls brain (Sv129-FVB). Brainstem, cerebellum and olfactory bulb were removed and the brain cut sagittal. One half was used for UHPLC-MS/MS lipidomic analysis. Lipid expression values (AUC divided by the AUC of the internal standard; AUC /IS) were square root transformed and auto-scaled to have a common mean and variance of 1 [Z score = (x- \bar{x})/SD]. Lipids were clustered according to Euclidean distance metrics using the Ward method. For easier evaluation, lipid species belonging to the same class are depicted in colour. Columns clustered in two clusters according to genotypes. The bottom line shows the IDs of individual mice (n = 10 Sv129FVB controls, n = 13 Pink1^{-/-}SNCA^{A53T} double mutant PD mice).

Suppl. Fig. 4



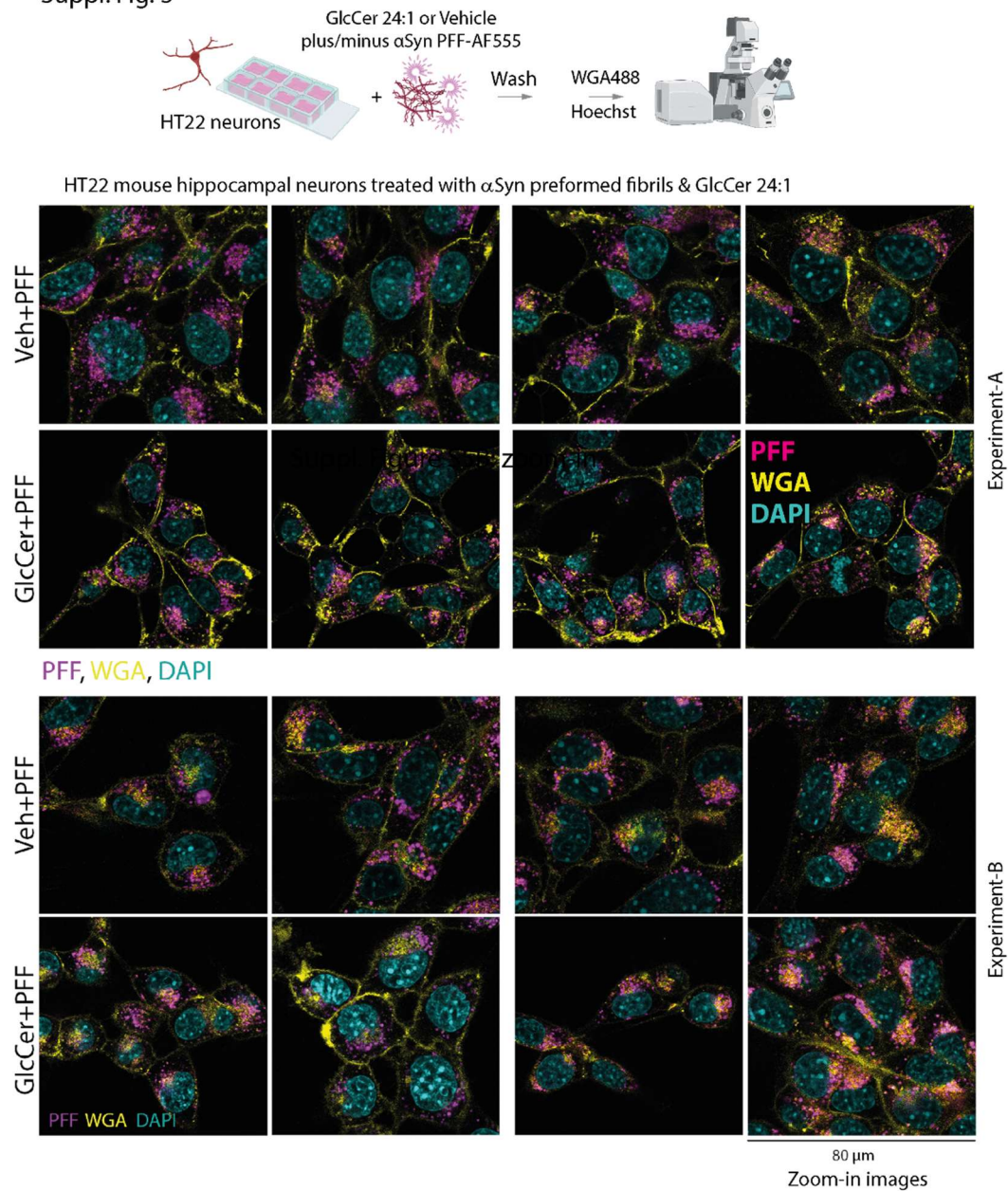
Supplementary Figure S4

HT22 mouse hippocampal neurons viability treated with alpha synuclein preformed fibrils (PFF)

A, B: HT22 were seeded into 96-well plates in the presence or absence of α Syn-PFF and GlcCer24:1, and the WST (water soluble tetrazolium) assay was performed 48h after seeding. The decrease of absorbance values was transformed into percentages of cell death. The data in A and B are each from two consecutive independent experiments. Scatters are replicates, the box is the interquartile range, the line is the median, whiskers show minimum to maximum. Errors bars in B are SD. α Syn-PFF per se had no impact on cell viability, but in combination with GlcCer 24:1 the fraction of cell death was increased.

C: Treatment of HT22 with α Syn-PFF caused a shift of phosphatidylcholine species from long-chain PC to short-chain PC. Z-scores of AUC/IS values were submitted to ANOVA and subsequent posthoc t-tests using an FDR adjustment of alpha. Asterisks show significant discoveries.

Suppl. Fig. 5



Supplementary Figure S5

Cellular uptake of preformed alpha synuclein fibrils (α Syn-PFF) in HT22 cells

Corresponding to figure 5 (main body) the images show zoom-in images of the uptake of AF555-labeled α Syn preformed fibrils in HT22 mouse hippocampal neurons. The images are each 4 examples taken at early and late time points in two independent consecutive replicate experiments. Pretreatment with GlcCer24:1 (1 μ M) had no significant impact on the PFF-AF555 fluorescence uptake in HT22 cells.

Suppl. Figure 6

β-Arrestin assay of candidate GPCR in HEK293 cells

Fold change versus average of vehicle (0 μM)																						
GlcCer18:1	ADORA1				ADRA2B				CHRM3				GPR63				GPR75					
0 μM	0.81	1.29	1.14	0.76	0.95	0.85	1.38	0.82	0.91	1.27	0.89	0.93	1	0.56	1.54	0.91	0.87	0.79	1.1	1.24		
1 μM	2.4	1.77	2.57	0.84	0.69	0.82	0.6	0.93	0.69	0.65	1.32	2.37	0.89	0.8	1.95	1.35	1.11	0.99	0.53	0.61		
5 μM	1.05	1.88	0.73	1.49	1.73	0.98	0.53	0.89	0.67	3.76	0.89	0.53	1.92	0.83	1.37	0.96	0.69	0.95	1.36	1.22		
10 μM	0.97	1.4	1.66	0.9	0.73	1.18	1.04	0.78	0.89	1.37	0.67	0.62	0.97	0.98	1.01	0.91	0.94	0.74	1.36	0.91		

GlcCer18:1	HRH1				HRH4				LPAR1				NPBW2				OXGR1				P2RY1			
0 μM	0.65	0.85	1.7	0.8	1.09	1.24	0.84	0.84	0.86	0.51	1.58	1.05	0.83	0.94	1.21	1.02	0.68	0.5	1.35	1.47	0.35	0.33	1.71	1.61
1 μM	0.65	1	2.25	1.22	2.06	1.22	0.53	1.37	1.33	0.99	1.41	0.76	1.07	1.44	6.61	2.65	0.88	0.96	1.26	1.31	1.65	1.62	1.02	1.88
5 μM	0.67	0.61	1.99	2.03	2.46	1.24	0.79	2.26	0.76	0.34	2.08	0.75	1.17	1.74	2.14	1.73	0.92	0.65	1.53	1.06	0.49	0.32	1.37	1.8
10 μM	1.45	0.48	0.77	0.93	4.13	1.76	1.25	1.13	1.95	0.88	0.79	0.29	2.46	1.25	1.9	2.03	1.19	0.47	1.2	0.99	1.97	1.76	0.42	0.43

Fold change versus average of vehicle (0 μM)																								
GlcCer24:1	GAL1				GRM5				MRGPRF				OPRL1				SSTR4				P2RY1			
0 μM	0.89	1.3	0.74	1.07	1.19	0.82	1.1	0.89	0.69	1.61	0.9	0.8	0.63	0.73	1	1.64	0.63	1.13	1.01	1.24	0.77	0.23	1.29	1.71
1 μM	0.35	0.62	0.25	0.61	0.42	0.52	0.41	0.52	0.83	0.8	0.9	1.11	1.74	1.27	1.15	1.92	1.03	0.78	0.71	1.05	0.33	0.49	4.73	0.75
5 μM	0.39	0.67	0.37	1.19	0.7	0.55	0.61	0.94	1.54	1.49	0.76	1.37	1.71	2.22	1.27	1.64	0.55	0.95	1.8	1.1	0.34	1.2	4.5	1.98
10 μM	0.67	1	0.75	1.02	0.72	1.19	1.41	2.1	1.75	1.63	2.41	2.13	2.81	2.83	3.08	3.96	1.38	1.83	1.19	2.58	4.36	0.25	1.29	1.94

Positive control - Muscarin receptor stimulation carbachol												Positive control - Muscarin receptor stimulation carbachol															
CHRM1				CHRM5				Untransfected				CHRM1				CHRM5				Untransfected							
0 μM	0.84	0.84	0.72	1.59	0.92	1.02	1.13	0.92	0.92	0.87	1.32	0.89	0.7	0.51	2.07	0.72	0.71	0.45	1.03	1.82	0.96	1.64	0.72	0.68			
1 μM	Experiment GlcCer18:1								0.56	0.94	0.78	0.99	Experiment GlcCer24:1								0.32	1.28	0.56	1			
5 μM									0.73	1.2	0.8	1.48									0.96	0.8	1.72	1.12			
10 μM									1.6	1.04	0.78	1.22									1.6	3.6	2.04	2.56			
100 μM	43.6	35.6	67.3	47.8	5.09	3.92	4.59	5.24					51.8	52.7	44.8	37.6	6.16	6.81	6.71	6.97							

Supplementary Figure S6

Replicates analyses of beta arrestin-based GPCR screening assay

GPCR activity was assessed in a heterologous expression model in COS cells stimulated with GlcCer 18:1 versus vehicle or GlcCer 24:1 versus vehicle at 1, 5 and 10 μM. The heatmap shows replicate analyses of GPCR candidates which were selected from an initial screen (330 GPCRs, 8 neg and 4x2 pos controls).